

Controlled growth of carbon nanotubes over cobalt nanoparticles by thermal chemical vapor deposition

Yoon Huh,^a Jeong Yong Lee,*^a Jinwoo Cheon,^b Young Kyu Hong,^c Ja Yong Koo,^c Tae Jae Lee^d and Cheol Jin Lee*^d

^aDepartment of Materials Science and Engineering, Korea Advanced Institute of Science and Technology, Daejeon 305-701, Korea. E-mail: jy.lee@kaist.ac.kr; Fax: +82-42-869-4276; Tel: +82-42-869-4216

^bDepartment of Chemistry, Yonsei University, Seoul 120-749, Korea

^cKorea Research Institute of Standards and Science, Daejeon 305-600, Korea

^dDepartment of Nanotechnology, Hanyang University, Seoul 133-791, Korea. E-mail: cjlee@hanyang.ac.kr; Fax: +82-2-2290-0768; Tel: +82-2-2293-4744

Received 25th April 2003, Accepted 25th June 2003

First published as an Advance Article on the web 16th July 2003

Controlled growth of carbon nanotubes (CNTs) has been achieved by thermal chemical vapor deposition of acetylene gas over nanometer-sized cobalt particles. The well-aligned CNTs, which have a uniform diameter and high purity, are synthesized over cobalt nanoparticles distributed on substrates of large area. The alignment, density, and diameter of the CNTs are easily controlled by adjusting the density of the cobalt nanoparticles. Moreover, growth rate, density, diameter, and crystallinity of CNTs grown over the cobalt nanoparticles are also well controlled by the growth temperature. Our results demonstrate that the controlled growth of CNTs can be effectively realized by adjusting cobalt nanoparticles and growth temperature.

1. Introduction

Carbon nanotubes (CNTs), since their first discovery in 1991,¹ have received much attention owing to their many potential technological applications arising from their extraordinary mechanical and electrical properties.^{2,3} CNTs have been synthesised using various methods, such as arc discharge,⁴ laser vaporization,⁵ pyrolysis,^{6,7} plasma-enhanced⁸ or thermal chemical vapor deposition (CVD).⁹ Of these, the CVD method allows the alignment, the density, and the diameter of CNTs to be controlled.⁸⁻¹⁵ Controlled growth of CNTs has potential for many useful applications in electronic devices and composite materials. By the way, for the synthesis of CNTs using the CVD method, it is necessary to prepare catalyst nanoparticles on a substrate during^{16,17} or before the synthesis of the CNTs. In order to form nanometer-sized catalyst particles on the substrate, various methods have been used, such as direct nanoparticle formation on the substrate,¹⁶⁻²¹ electrodeposition,²² film deposition followed by etching^{8,12,23} or thermal annealing,^{24,25} and nanoparticle dispersion.^{11,14,15,26,27} Flahaut *et al.*¹⁶ attained a very homogeneous dispersion of nanoparticles by using *in situ* formation of the catalyst nanoparticles during the CVD process. Recently, the nanoparticle dispersion method was also proven to control the diameter and density of catalyst particles over a wide area of various substrates.^{11,14,27} Some research groups have reported that the diameter of CNTs could be controlled by the size or density of the catalyst nanoparticles uniformly distributed on various substrates.^{12,14,19,25,26} However, there has been no reports on the control of the alignment and density of CNTs over catalyst nanoparticles dispersed on the substrates.

Here, we report that the alignment, density, and diameter of CNTs can be effectively controlled by adjusting the density of cobalt nanoparticles dispersed on Si substrate. We also demonstrate that the growth rate, density, diameter, and crystallinity of CNTs grown over catalyst nanoparticles can be controlled by varying the growth temperature. We suggest that the controlled growth of CNTs can be easily performed by our method.

2. Experimental

The Co nanoparticles were synthesized by a thermal decomposition process and dispersed on Si substrates using the spin-coating method.^{27,28} We prepared colloidal solutions by dispersing AOT-stabilized [AOT = bis(2-ethylhexyl) sulfosuccinate] Co nanoparticles in toluene. After varying the molar concentration of colloids by dilution (1 mM, 20 mM, and 80 mM), the conventional spin-coating method was employed to spread the Co nanoparticles over a wide area of n-type Si substrates. The spin-coater was rotated at 5000 rpm for 30 min.

To study the growth properties of CNTs over Co nanoparticles, we synthesized CNTs in the temperature range of 750–950 °C. The nanoparticle-spread Si substrates, which were prepared from 1, 20, and 80 mM colloids, were mounted in the quartz tube of the thermal CVD system, and the quartz tube was then heated to the growth temperature in a flow of Ar at 1000 sccm. After arriving at the desirable growth temperature, the Ar gas flow was replaced by C₂H₂ gas with a flow rate of 30 sccm for 10 min at the same temperature for the synthesis of CNTs. After the reaction, the quartz tube was cooled to room temperature in ambient Ar.

Scanning electron microscopy (SEM, Hitachi, S-4700) was used to investigate the distribution of Co nanoparticles and the morphology of the CNTs. Transmission electron microscopy (TEM, JEOL, JEM 2000 EX) was used to investigate the structure and crystallinity of the CNTs. In addition, the overall crystallinity of the CNTs was characterized by Raman spectroscopy (Renishaw, Micro-Raman 2000). The 514.5 nm line of an Ar laser was used for excitation.

3. Results and discussion

Fig. 1 shows the SEM images of Co nanoparticles distributed on the Si substrate by the spin-coating method. The Co nanoparticles are very uniformly distributed on silicon substrates by spin-coating from their colloidal solutions. The molar concentrations of colloidal solutions prepared in this work were

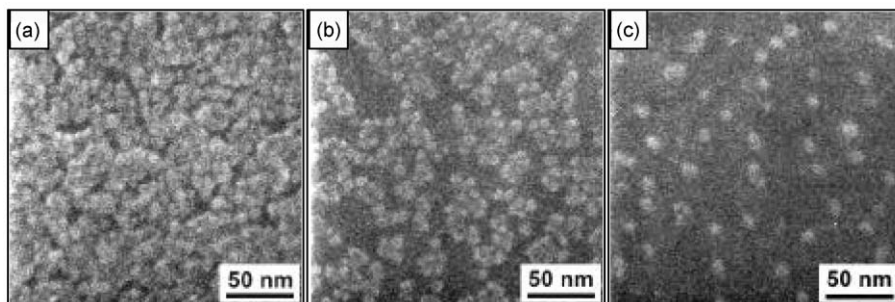


Fig. 1 The SEM images of Co nanoparticles distributed on the silicon substrate. (a) 80 mM colloidal solution, (b) 20 mM colloidal solution, and (c) 1 mM colloidal solution.

80 mM [Fig. 1(a)], 20 mM [Fig. 1(b)], and 1 mM [Fig. 1(c)]. The Co nanoparticles, which have an average diameter of 8 nm, are uniformly distributed on the Si substrate regardless of the nanoparticle density. The densities of Co nanoparticles are estimated to be $1.9 \times 10^{12} \text{ cm}^{-2}$ [Fig. 1(a)], $6.0 \times 10^{11} \text{ cm}^{-2}$ [Fig. 1(b)], and $1.1 \times 10^{11} \text{ cm}^{-2}$ [Fig. 1(c)] from the SEM images. The density of Co nanoparticles increases with increasing molar concentration of the colloidal solution. It is noteworthy that the Co nanoparticles are fairly uniformly distributed over a wide area of the substrates, indicating that the density of the nanoparticles is easily controllable by adjusting the molar concentration of the nanoparticle colloidal solution.²⁷

Fig. 2 shows the SEM images of CNTs grown at 850 °C over the Co nanoparticles distributed on the Si substrate. Fig. 2(a) shows that in the case of high-density Co nanoparticles, high-density CNTs are synthesized with good alignment on the Si substrate. On the other hand, low-density CNTs are produced with poor alignment in the case of the low-density Co nanoparticles as shown in Fig. 2(b). Moreover, rare CNTs are partly synthesized on the Si substrate in the case of very low density of Co nanoparticles as shown in Fig. 2(c). It is well known that the alignment of CNTs synthesized by thermal CVD is mainly dependent on the steric hindrance of the neighbouring CNTs.²⁹ In this work, vertical alignment of CNTs can be achieved when the density of catalyst particles reaches a certain density (over $1.9 \times 10^{12} \text{ cm}^{-2}$). In Fig. 2(d)–(f), the magnified SEM images of the top-views of the CNTs show that the CNTs have a uniform diameter of about 30 nm irrespective of Co nanoparticle density, resulting from the uniform size of the Co nanoparticles. Our result indicates that the alignment and density of CNTs can be controlled by adjusting the density of Co nanoparticles.

We investigated the effect of temperature on CNT growth over Co nanoparticles. Fig. 3 shows the SEM images of CNTs grown at 750, 850, and 950 °C over Co nanoparticles with a density of $1.9 \times 10^{12} \text{ cm}^{-2}$. The vertically well-aligned CNTs were homogeneously synthesized on the Si substrate regardless of the growth temperature. In Fig. 3(a)–(c), the average lengths of the CNTs at 950, 850, and 750 °C are about 30 μm , 6 μm , and 2 μm , respectively. The higher the growth temperature is, the more enhanced the rate of CNT growth. Besides the kinetics of carbon, we consider that the diffusion and reaction rate of carbon atoms increase with increasing growth temperature. This result is similar to that of our previous work in which CNTs were grown over a Fe catalytic film deposited on Si substrate by thermal CVD.¹²

Fig. 3(d)–(f) show the magnified SEM images of the top-views of vertically aligned CNTs. The average diameter of the CNTs increases as the temperature increases from 750 to 950 °C, while the density of the CNTs decreases. The densities of the CNTs grown at 950, 850, and 750 °C are $\sim 2.1 \times 10^9 \text{ cm}^{-2}$, $\sim 7.6 \times 10^9 \text{ cm}^{-2}$, and $\sim 9.5 \times 10^9 \text{ cm}^{-2}$, respectively. As the growth temperature increases, the migration rate of Co nanoparticles on the Si surface increases, resulting in active agglomeration of Co nanoparticles. As a result of this agglomeration at higher temperatures during the thermal CVD process, the size of the Co nanoparticles increases but their density decreases. It is well understood that the diameter of CNTs usually depends on the size of the catalytic particles in CVD growth.

We observed TEM images of the CNTs synthesized over Co nanoparticles with a density of $1.9 \times 10^{12} \text{ cm}^{-2}$. Fig. 4 shows that the CNTs produced at all three temperatures are multiwalled carbon nanotubes (MWNTs). The MWNTs have a

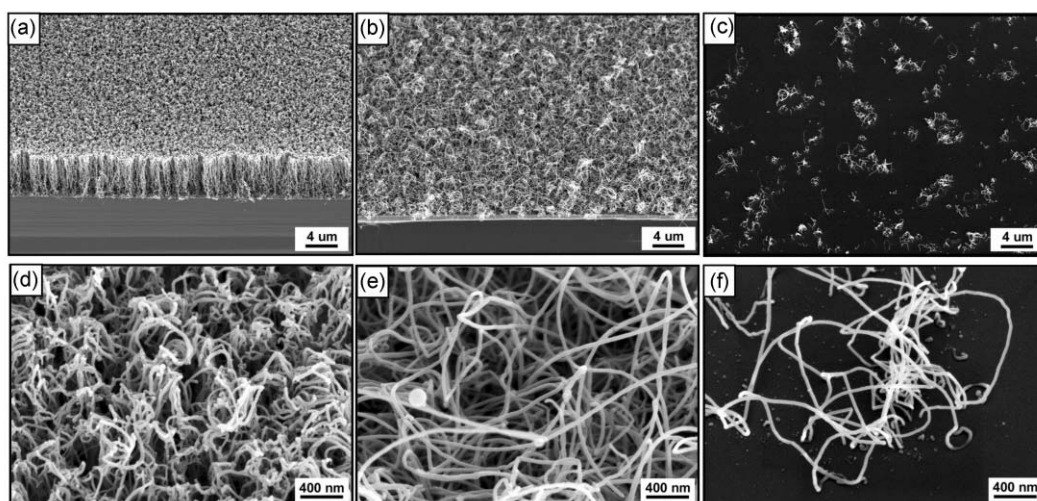


Fig. 2 The SEM images of CNTs grown over Co nanoparticles by thermal CVD of C_2H_2 at 850 °C. (a)–(c) Low-magnification SEM images of CNTs and (d)–(f) high-magnification SEM images of the top-views of CNTs. (a), (d) Co nanoparticle density: $1.9 \times 10^{12} \text{ cm}^{-2}$; (b), (e) Co nanoparticle density: $6.0 \times 10^{11} \text{ cm}^{-2}$; and (c), (f): $1.1 \times 10^{11} \text{ cm}^{-2}$.

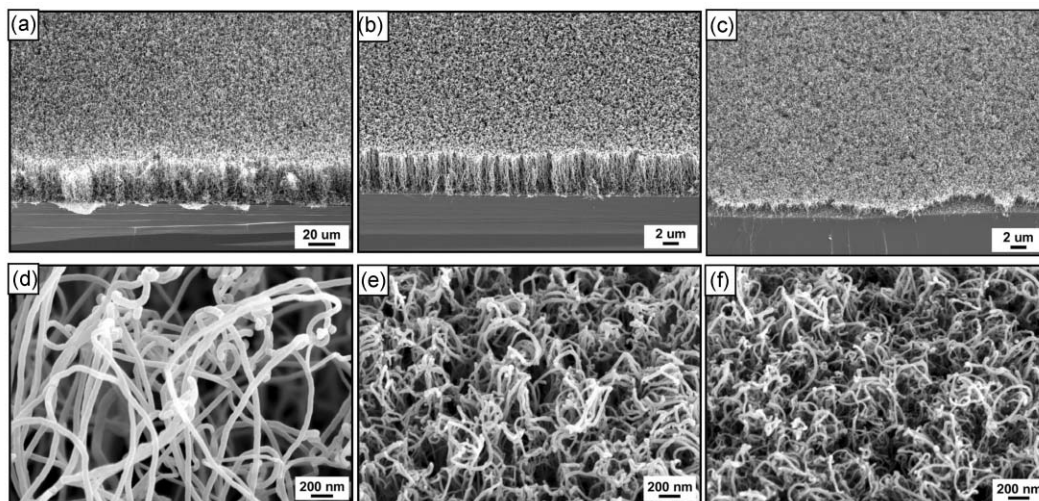


Fig. 3 The SEM images of CNTs grown over Co nanoparticles with a density of $1.9 \times 10^{12} \text{ cm}^{-2}$ by thermal CVD of C_2H_2 . (a), (d) At 950 °C; (b), (e) at 850 °C; and (c), (f) at 750 °C. (a)–(c) Vertically well-aligned CNTs on the silicon substrate and (d)–(f) top-views of the well-aligned CNTs.

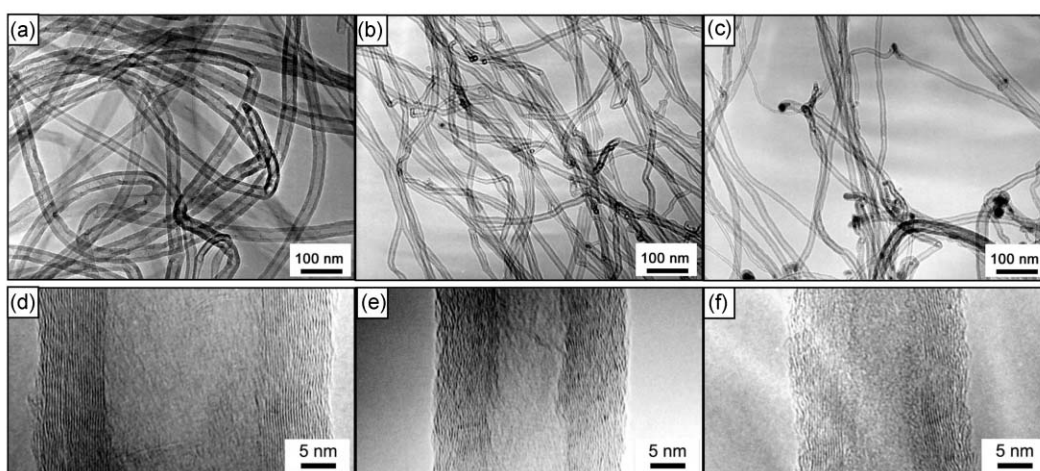


Fig. 4 The TEM images of MWNTs grown over Co nanoparticles with a density of $1.9 \times 10^{12} \text{ cm}^{-2}$ by thermal CVD of C_2H_2 . (a), (d) At 950 °C; (b), (e) at 850 °C; and (c), (f) at 750 °C. (a)–(c) Low-magnification TEM images and (d)–(f) HRTEM images.

bamboo-like structure as shown in Fig. 4(a). Sometimes, at the low growth temperature of 750 °C the closed ends of the MWNTs have encapsulated Co nanoparticles as shown in Fig. 4(c). Fig. 4(a)–(c) show that the MWNTs have uniform diameters of about 40, 30, and 25 nm at 950, 850, and 750 °C, respectively. This result indicates that a very uniform diameter of CNTs can be attained using Co nanoparticles and that the diameter and density of the CNTs can also be controlled by adjusting the growth temperature. Fig. 4(d)–(f) show high-resolution TEM (HRTEM) images of MWNTs grown at 950, 850, and 750 °C, respectively. As illustrated in Fig. 4(d), the MWNTs grown at 950 °C have clear fringes of graphitic sheets separated by 0.34 nm. The HRTEM images in Fig. 4(e)–(f) show the MWNTs grown at 850 and 750 °C have a poor crystallinity compared with those grown at 950 °C. HRTEM observations indicate that the crystallinity of CNTs improves as the growth temperature increases. The outer graphitic sheets have a more defective structure than that of the inner graphitic sheets. We consider that the defective outer graphitic shells are caused by non-catalytic thickening of the CNTs during CNT growth. In general, the outer graphitic shells are less catalyzed than the inner ones, resulting in the outer shells being more defective.

Fig. 5 shows the first-order Raman spectra of the as-grown CNTs. All spectra show mainly two Raman bands at approximately 1336 cm^{-1} (D-band) and 1582 cm^{-1} (G-band), which are characteristic of a disordered and sp^2 -hybridized carbon

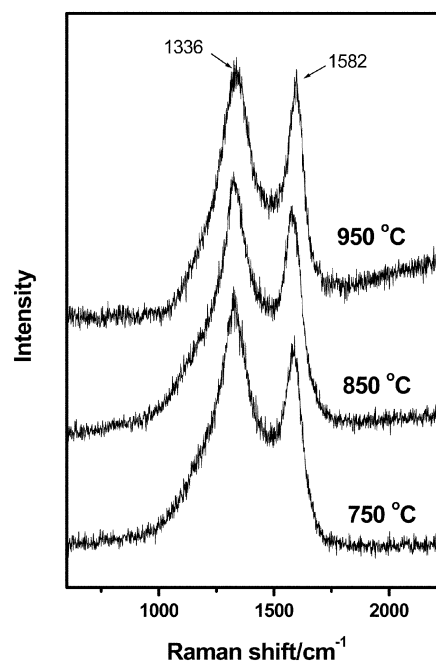


Fig. 5 First-order Raman spectra of as-grown CNTs at 750, 850, and 950 °C over Co nanoparticles. The 514.5 nm line of an Ar laser was used for excitation.

material, respectively. In general, the G-band indicates highly crystalline graphitic layers, while the D-band reveals the existence of defects in the graphitic layer.^{30,31} Therefore, the strength of the G-band relative to the D-band is a measure of the amount of crystallinity in the carbon materials.³⁰ In this work, the strength of the D-band relative to the G-band decreases as the growth temperature increases. This result indicates that the crystallinity of the graphitic sheets progressively improves as the growth temperature increases, which is consistent with the HRTEM images.

4. Conclusion

In summary, we have demonstrated the synthesis of MWNTs with a bamboo-like structure over Co nanoparticles distributed on Si substrates by thermal CVD of C₂H₂ gas. The alignment, density, and diameter of the CNTs could be controlled by adjusting the density of the Co nanoparticles dispersed on the Si substrate. Moreover, the growth rate, diameter, density, and crystallinity of the CNTs could also be controlled by adjusting the growth temperature. The CNTs grown over the Co nanoparticles had a very uniform diameter and density. We suggest that our method is a very simple and effective way to realize the controlled growth of CNTs on various substrates, which is very promising for the many applications that use CNTs.

Acknowledgements

This work was supported by the Ministry of Science and Technology of Korea through the National Research Laboratory Program, by the Center for Nanotubes and Nanostructured Composites at SKKU, and by the National R&D project for Nanoscience and Technology of MOST.

References

- 1 S. Iijima, *Nature*, 1991, **354**, 56.
- 2 P. M. Ajayan, O. Stephan, C. Colliex and D. Trauth, *Science*, 1994, **265**, 1212.
- 3 W. A. de Heer, A. Chatelain and D. Ugarte, *Science*, 1995, **270**, 1179.
- 4 D. S. Bethune, C. H. Kiang, M. S. De Vries, G. Gorman, R. Savoy, J. Vazquez and R. Beyers, *Nature*, 1993, **363**, 605.
- 5 A. Thess, R. Lee, P. Nikolaev, H. Dai, P. Petit, J. Robert, C. Xu, Y. H. Lee, S. G. Kim, A. G. Rinzler, D. T. Colbert, G. E. Scuseria, D. Tomanek, J. E. Fisher and R. E. Smalley, *Science*, 1996, **273**, 483.
- 6 M. Terrones, N. Grobert, J. Loivates, F. P. Zhang, H. Terrones,

- N. Kordatos, W. K. Hsu, J. P. Hare, P. D. Townsend, K. Prassides, A. K. Cheetham, H. W. Kroto and D. R. M. Walton, *Nature*, 1997, **388**, 52.
- 7 R. Sen, A. Govindaraj and C. N. R. Rao, *Chem. Phys. Lett.*, 1997, **267**, 276.
- 8 Z. F. Ren, Z. P. Huang, J. W. Xu, J. H. Wang, P. Bush, M. P. Siegal and P. N. Provencio, *Science*, 1998, **282**, 1105.
- 9 S. Fan, M. G. Chapline, N. R. Franklin, T. W. Tombler, A. M. Cassell and H. Dai, *Science*, 1999, **283**, 512.
- 10 C. N. R. Rao, R. Sen, B. C. Satishkumar and A. Govindaraj, *Chem. Commun.*, 1998, 1525.
- 11 H. Ago, T. Komatsu, S. Ohshima, Y. Kuriki and M. Yumura, *Appl. Phys. Lett.*, 2000, **77**, 79.
- 12 C. J. Lee, J. Park, Y. Huh and J. Y. Lee, *Chem. Phys. Lett.*, 2001, **343**, 33.
- 13 Z. Zhang, B. Q. Wei and P. M. Ajayan, *Appl. Phys. Lett.*, 2001, **79**, 4207.
- 14 C. L. Cheung, A. Kurtz, H. Park and C. M. Lieber, *J. Phys. Chem. B*, 2002, **106**, 2429.
- 15 K.-H. Lee, J.-M. Cho and W. Sigmund, *Appl. Phys. Lett.*, 2003, **82**, 448.
- 16 E. Flahaut, A. Govindaraj, A. Peigney, Ch. Laurent, A. Rousset and C. N. R. Rao, *Chem. Phys. Lett.*, 1999, **300**, 236.
- 17 R. K. Rana, Y. Kolytynin and A. Gedanken, *Chem. Phys. Lett.*, 2001, **344**, 256.
- 18 O. A. Nerushev, M. Sveningsson, L. K. L. Falk and F. Rohmund, *J. Mater. Chem.*, 2001, **11**, 1122.
- 19 Y. Li, W. Kim, Y. Zhang, M. Rolandi, D. Wang and H. Dai, *J. Phys. Chem. B*, 2001, **105**, 11424.
- 20 H. C. Choi, S. Kundaria, D. Wang, A. Javey, Q. Wang, M. Rolandi and H. Dai, *Nano Lett.*, 2003, **3**, 157.
- 21 C. Emmenegger, J.-M. Bonard, P. Mauron, P. Sudan, A. Lepora, B. Grobety, A. Züttel and L. Schlapbach, *Carbon*, 2003, **41**, 539.
- 22 Y. Tu, Y. Lin and Z. F. Ren, *Nano Lett.*, 2003, **3**, 107.
- 23 C. J. Lee, D. W. Kim, T. J. Lee, Y. C. Choi, Y. S. Park, W. S. Kim, Y. H. Lee, W. B. Choi, N. S. Lee, J. M. Kim, Y. G. Choi and S. C. Yu, *Appl. Phys. Lett.*, 1999, **75**, 1721.
- 24 Y.-H. Lee, Y.-T. Jang, D.-H. Kim, J.-H. Ahn and B.-K. Ju, *Adv. Mater.*, 2001, **13**, 479.
- 25 O. A. Nerushev, S. Dittmar, R.-E. Morjan, F. Rohmund and E. E. B. Campbell, *J. Appl. Phys.*, 2003, **93**, 4185.
- 26 Y. Li, J. Liu, Y. Wang and Z. L. Wang, *Chem. Mater.*, 2001, **13**, 1008.
- 27 Y. K. Hong, H. Kim, G. Lee, W. Kim, J. I. Park, J. Cheon and J. Y. Koo, *Appl. Phys. Lett.*, 2002, **80**, 844.
- 28 J. I. Park, N. J. Kang, Y. W. Jun, S. J. Oh, H. C. Ri and J. Cheon, *Chem. Phys. Chem.*, 2002, **3**, 543.
- 29 C. J. Lee, D. W. Kim, T. J. Lee, Y. C. Choi, Y. S. Park, Y. H. Lee, W. B. Choi, N. S. Lee, G. S. Park and J. M. Kim, *Chem. Phys. Lett.*, 1999, **312**, 461.
- 30 P. C. Eklund, J. M. Holden and R. A. Jishi, *Carbon*, 1995, **33**, 959.
- 31 M. Sveningsson, R. E. Morjan, O. A. Nerushev, Y. Sato, J. Bäckström, E. E. B. Campbell and F. Rohmund, *Appl. Phys. A*, 2001, **73**, 409.